PCCP

Accepted Manuscript




ROYAL SOCIETY OF CHEMISTRY

www.rsc.org/pccp

# Theoretical Tools to Distinguish *O*-Ylides from *O*-Ylidic Complexes in Carbene-Solvent Interactions

Sara Gómez,* Albeiro Restrepo, and C. Z. Hadad*

*Grupo de Química–Física Teórica, Instituto de Química, Universidad de Antioquia, Calle 70 No. 52-21, Medellín, Colombia.*

E-mail: sluz.gomez@udea.edu.co; cacier.hadad@udea.edu.co

*To whom correspondence should be addressed

**Abstract**

In this paper, we report the geometries and properties of 48 molecular species located on the MP2/6-311++G$(d,p)$ PES of the fluorocarbene-(methanol)$_3$ system. The structures were found by a combination of a stochastic search method, using a modified Metropolis acceptance test, and some hand constructed very symmetrical structures. We use several theoretical descriptors to categorize these species, focusing our attention in the interaction between the carbene carbon and the methanol oxygen, Cc$\cdots$O, because this is the key interaction in the formation of *O*-ylides, ether products, and *O*-ylidic solvation complexes. These descriptors include natural charges and natural bond orbitals (NBO), Cc$\cdots$O bond orders, Cc$\cdots$O distances, energetic stabilities, and properties at bond critical points. Accordingly, the isomers were divided into four groups: ethers, fluorocarbene–methanol *O*-ylides, *O*-ylidic carbene-solvent complexes and hydrogen bonded carbene–solvent complexes. We found that the possibility of forming H-bonds among solvent molecules and between the carbene carbon and the hydrogen of the solvent molecule affects the stability, structure and nature of Cc$\cdots$O interactions in *O*-ylides and *O*-ylidic complexes to the point of generating some diffuse borderline between these two kinds of species. We established what set of theoretical tools is suitable to better distinguish between them. Additionally, we clarify the nature of the relevant interactions in these species.

**Keywords**: Carbenes solvation. NBO analysis. QTAIM analysis. Carbene-Solvent Interactions. Ylides. *O*-ylidic Complexes. Singlet Fluorocarbene, Transient Specific Solvation.

# Introduction

Carbenes, X–C̈–Y, are substances usually acting as reaction intermediates.[1,2] Since the postulation of their existence in 1903[3] and the discovery of their role as intermediates in chemical reactions, carbenes have been employed in a wide variety of versatile and useful organic and inorganic syntheses.[4–6]

Carbenes are electron deficient species with a pair of non-bonding electrons. They are known to exist in two different electronic spin states. One of them is the triplet, with two unpaired electrons, one occupying an $sp^2$-like orbital and the other occupying a *p*-like orbital on the carbon atom. The other state is singlet, where the pair of non-bonding electrons occupy an $sp^2$-like orbital, while the *p*-like carbene carbon orbital remains empty.[7] The singlet-triplet (S-T) energy gap and relative stability depend on a number of factors, such as the nature of the substituents on the carbon atom, chemical environment, solvents, among others.[8–10] As a general rule, the triplet state is the lowest energy state, nevertheless several substituents are able to stabilize the singlet state inverting the S-T gap. Examples are -$NR_2$, -OR, -F, -Cl, -Br, -I,[6] among others. Recent studies have shown that once generated, ground state singlet carbenes can be temporarily stabilized by means of the formation of *meta*-stable complexes with solvent molecules having nonbonding electrons (examples: oxygen atom in ethers or alcohols) or $\pi$ electrons (examples: benzene, aromatic rings).[11–13] The stabilization would ocurr through the interaction between the excess electron density in solvent molecules and the empty *p*-like orbital in the carbene carbon atom.[14]

Singlet carbenes can be generated from photolysis of diazirines[15,16] using Laser Flash Photolysis (LFP).[17] In this technique, a light pulse is used to excite the sample and to generate transient species (carbenes in this case) suitable for spectroscopic observation.[18] The combination of LFP and ultrafast spectroscopy methods[9] (IR, UV-Vis) has allowed researchers to register time dependent transformations of carbenes and to detect carbene-solvent metastable complexes just before the

system evolves towards the formation of final reaction products, such as ylides, ethers or cyclopropanes. Methylchlorocarbene, benzilchlorocarbene,[19] $p-$nitrophenylchlorocarbene,[20] chlorocarbene amide,[14] and dichlorocarbene[21] are among those carbenes whose complexation with solvents such as dioxane, tetrahydrofuran, anisole, some methylanisoles, 1,3-methoxybenzene, 1,3,5-methoxybenzene, etc., has been detected.

An usual consequence of complexation is the alteration of carbene reactivity. For example, it has been experimentally found that the formation of complexes extends the lifetime of carbenes,[22] changes the selectivity in insertions toward O–H groups,[23] modulates rearrangement products[24] and decreases the reaction constants of addition to olefins or of the ylides formation.[19,25]

All of the above mentioned findings were supported by computational calculations[26,27] in which the metastable species were described from proposed 1:1 carbene:solvent molecular complexes. In general, the suggested complexes are of $\pi-$type and of $O-$ylidic-type,[20,28,29] in which the carbene carbon interacts with the $\pi$ system or with the oxygen lone pair of the solvent molecule, respectively. In such complexes, carbene–solvent interactions are shown to be weak.[19]

Experimental evidence[14] showing the simultaneous action of two or more solvent molecules in the complexation process and the fact that the structure of the complexes are usually postulated using the chemical intuition of the researchers, highlight the need to introduce new and more efficient methods of structure searching and for the exploration of the Potencial Energy Surfaces (PES) for the title systems. For that purpose, it has been shown to be helpful to combine hand constructed and stochastic sampling methodologies in the case of complexes among fluorocarbene amide and two tetrahydrofuran molecules.[30]

One of the stochastic sampling methods is ASCEC (Annealing Simulado con Energía Cuántica). This algorithm[31–33] has been designed to produce sets of suitable cluster candidate structures

to be subjected to further optimization using traditional gradient-following techniques. ASCEC applies a modified Metropolis acceptance test in an adapted version of the simulated annealing optimization procedure,[34,35] which allows to conserve the comparative advantages of stochastic optimization over analytical methods.[36] The ASCEC method has been successfully used to treat diverse systems,[37–54] and is used in this work. Further details about this methodology can be found elsewhere.[32,33]

One problem in the case of *O*-ylidic species is the distinction between *O*-ylidic solvation complexes and *O*-ylide products. As mentioned by Moss,[22] *O*-ylide products consist in species with fully developed C-O single bonds with typical oxygen-carbon bond lengths (around 1.5 Å[21]), while in *O*-ylide transient complexes the C-O separation is significantly longer than in typical C-O bonds (for example, around 2.2 Å for dichlorocarbene-THF complex[21]). However, if what is intended is to perform an as exhaustive as possible scan of the configurational space of a carbene-solvent system, one encounters potential energy surfaces populated with many local minima, including structures with an intermediate character between *O*-ylides and *O*-ylidic complexes. These species could be either transient species as well as species with considerable thermodynamic stability. A total exploration and characterization of the PES for carbene-solvent interactions would be useful in understanding the nature of the species formed in an experimental system where singlet carbenes are generated in the presence of solvent molecules containing oxygen atoms. We are interested in the specific solvation of singlet carbenes with solvent molecules containing electron-donor oxygen atoms (electron lone pairs). In these cases, the transient metastable carbene-solvent complexes formed before the final products of the reaction, are of *O*-ylidic-type. The final products of the reactions can be *O*-ylides or ethers, in the case of using alcohols as solvent molecules.

In this paper, we attempt to characterize the potential energy surface (PES) for fluorocarbene–(methanol)$_2$ clusters. We use, among others, the tools provided by Bader's quantum theory of atoms in molecules (QTAIM),[55] and the concepts of Natural Bond Orbitals (NBO)[56] to study the nature of bonding,

and to elaborate a methodology to distinguish between *O*-ylides, *O*-ylidic-like complexes and intermediate cases (if any). Fluorocarbene (FC̈H), our singlet ground state carbene model has a singlet-triplet gap of -9 kcal/mol.[7] Methanol molecules, besides having oxygens with lone electron pairs to interact with the empty *p*-like carbene carbon orbital, can form hydrogen bonds through the interaction between the singlet carbene carbon $sp^2$ electron pair and its OH group. Three solvent molecules were chosen in order to allow the possibility of solvation from both sides of the carbene molecular plane, with simultaneous formation of hydrogen bonds of the MeOH···:CHF type. It is important to recognize that this system is by no means representative of a carbene generated in a real solution, but it is a model system which would allow us to increase the understanding of the carbene-solvent interactions, and would provide us with tools to tackle the problem with a more representative model.

# Computer methods

## Candidate clusters

Candidate structures for the FC̈H + 3MeOH system in overall singlet electronic state were generated through either random walks of the PES or hand constructed configurations. In the former case, the ASCEC program[31] was employed. All ASCEC runs were carried out using the big bang approach to construct the initial geometries: all flourocarbene and methanol molecules were placed at the same position and were allowed to evolve under the annealing conditions within a cube 7 Å of length. The stochastic samplings generated 427 candidate structures. Similar to a previous study,[30] in the hand constructing method, we considered the possible symmetric configurations, which are very difficult to find by a stochastic search method.

## Equilibrium geometries

Second order perturbation theory (MP2) in conjunction with the 6-311++g($d,p$) basis set was used to optimize and characterize the above mentioned candidate structures. This level of theory ensures a good treatment of electron correlation and appropriate description of the forces that are involved in the stabilization of the title clusters. It is worth mentioning that dispersion is important in this type of systems as mentioned by experimental and theoretical researchers,[30,57] who pointed out that when DFT is used, because of their parameterized nature, some properties are functional dependent, and that dispersion corrections are usually needed. We chose the basis set among other things, to include possible interactions between the hydrogen atoms of the methanol molecules and the doubly occupied $\sigma-$type carbene carbon orbital.[30] Characterization of stationary points as true minima was carried out by analyzing the results of harmonic frequencies calculations (no negative eigenvalues of the Hessian matrix), using the same level of theory. Highly correlated CCSD(T)/6-311++g($d,p$) energies[58] were calculated on all MP2 optimized geometries. Our choice of methodology has proven to be very accurate for the treatment of hydrogen-bonded clusters.[37–40,43–46]

Total binding energies (*BE*) were calculated by subtracting the sum of the energies of the constituting isolated moieties from the energy of a particular fluorocarbene–$(methanol)_3$ cluster. Thus, larger negative numbers correspond to larger stabilization energies. Relative binding energies ($\Delta BE$) at each level of theory, were obtained as the difference between the energy of the most stable ylide and the energy of a particular cluster on a given PES. All energies were corrected for the MP2/6-311++g$(d,p)$ zero-point vibrational energies (ZPE). We adopted the clusters stability order based on the CCSD(T)/6-311++g$(d,p)$//MP2/6-311++g$(d,p)$ $\Delta BE$ values. All optimization, frequency, and energy calculations were carried out using the *Gaussian 09* suite of programs.[59] Isomer populations were estimated by standard Boltzmann distribution analysis.

## Characterization of the structures

In order to analyze intermolecular bonding in fluorocarbene-$(methanol)_3$ clusters, the Quantum Theory of Atoms in Molecules (QTAIM) and the NBO method were used. For each true minimum, topological analysis of the electron density was carried out and a number of properties, such as electron density $\rho(\mathbf{r}_c)$, its Laplacian $\nabla^2\rho(\mathbf{r}_c)$ and the potential $\mathscr{V}(\mathbf{r}_c)$, and kinetic $\mathscr{G}(\mathbf{r}_c)$ energy densities, were calculated at the bond critical points (BCPs) for intermolecular interactions. We focused the analysis on the Cc(carbene carbon)–O(solvent) BCP, because the Cc$\cdots$O interaction dictates whether ylides or ethers are formed, and because Cc$\cdots$O is the relevant interaction in the formation of *O*-ylidic complexes.[14] BCPs are defined as a subset of points for which the gradient of the electron density vanishes, while being the point of minimum electron density in a bond path (BP). A BP is the line of maximum electron density connecting two interacting atoms. The bond critical points link adjacent nuclei via atomic interaction lines. The set of all atomic interaction lines ocurring in a given molecule constitutes the molecular graph.[60]

The pattern of bonding, within the QTAIM framework, is extracted by monitoring the values of the already mentioned properties at BCPs of interest. Large electron densities at BCPs are associated to high electron populations in the region between the pair of atoms, which correspond

to interactions with shared electrons and high degrees of covalency. This in turn leads to $\nabla^2\rho(\mathbf{r}_c) < 0$. Conversely, depletion of charge at the critical point, usually leads to smaller $\rho(\mathbf{r}_c)$ values and corresponds to positive Laplacians, $\nabla^2\rho(\mathbf{r}_c) > 0$, which are associated to closed shell interactions such as ionic bonds, hydrogen bonding, and long range interactions (in the case studied here, closed shell, weak, non-ionic interactions). Extreme cases of covalent bonds with low electron densities at the BCPs are known.[61]

A number of additional QTAIM properties are useful to characterize the bonding between two atoms.[62] One of them is the sign of the total energy density evaluated at BCPs, $\mathscr{H}(\mathbf{r}_c) = \mathscr{V}(\mathbf{r}_c) + \mathscr{G}(\mathbf{r}_c)$, where $\mathscr{G}(\mathbf{r}_c)$ and $\mathscr{V}(\mathbf{r}_c)$ are the associated kinetic and potential energy densities at BCPs, respectively. Even though $\nabla^2\rho(r_c) > 0$, if $\mathscr{H}(\mathbf{r}_c) < 0$ with $2 < |\mathscr{V}(\mathbf{r}_c)|/\mathscr{G}(\mathbf{r}_c) < 1$, bonding, although not properly covalent, has certain degree of covalency. This can be established by the criteria suggested by Espinosa and co-workers, in which the interactions can be discerned between covalent (or shared), closed shell, and intermediate type, according to the following scheme:[63]

$$\frac{|\mathscr{V}(\mathbf{r}_c)|}{\mathscr{G}(\mathbf{r}_c)} = \begin{cases} < 1, & \text{closed shell} \\ \in [1,2], & \text{intermediate} \\ > 2, & \text{covalent} \end{cases} \tag{1}$$

In this work, we calculate the $|\mathscr{V}(\mathbf{r}_c)|/\mathscr{G}(\mathbf{r}_c)$ and $\mathscr{H}(\mathbf{r}_c)/\rho(\mathbf{r}_c)$ ratios at Cc$\cdots$O BCPs for all equilibrium geometries. All topological properties of the electron densities were calculated using the AIMStudio suite of programs.[55]

Wiberg bond indices,[64] natural charges, natural resonance theory (NRT) bond orders and natural bonding orbitals (NBO) analyses were performed along the lines of the NBO program,[56] as

implemented in *Gaussian09*. As in the case of the electron density at the critical points for covalent bonds, the increase of bond orders values clearly indicates higher concentration of electrons between the interacting atoms and vice versa.

Second Order Perturbation Theory Analysis of the Fock Matrix within the NBO scheme was used to evaluate the donor-acceptor interactions.[65] The interactions result in a loss of occupancy from the localized NBO of an idealized Lewis structure into an empty non-Lewis orbital. For each donor ($i$) and acceptor ($j$), the stabilization energy $E^{(2)}$ associated with the $i \longrightarrow j$ delocalization is estimated as

$$E^{(2)} = \Delta E_{ij} = q_i \frac{[F(i,j)]^2}{\varepsilon_j - \varepsilon_i} \tag{2}$$

where $q_i$ is the occupancy of the donor orbital, $\varepsilon_i$ and $\varepsilon_j$ are orbital energies and $F(i,j)$ are the off-diagonal NBO Fock matrix elements.

At this point, we highlight the difference between primary (the donated proton comes from an O–H bond) and secondary (the donated proton comes from a C–H bond) hydrogen bonds, given the fact that the system chosen for this study contains three methanol solvent molecules and it is well known that alcohols are capable of forming hydrogen bonding networks.

# Results and discussion

## Structures, energies and stabilization

Equilibrium geometries for singlet [FCH(MeOH)$_3$] clusters were produced via the method outlined above. We found 48 equilibrium structures on the MP2/6-311++G$(d,p)$ PES when the ASCEC and hand constructing procedures were applied. Four groups can be described (see below in the Classification of clusters section): ethers, $e_n$, $O$-ylides, $y_n$, and complexes ($O$-ylidic-type and H-bonded-type), $c_n$. Their geometries, notation, and relative energies are shown in Figure 1, Figure 2, Figure 3 and Figure 4. Cartesian coordinates for all chemical species can be found in Appendix A4 of the supplementary material.

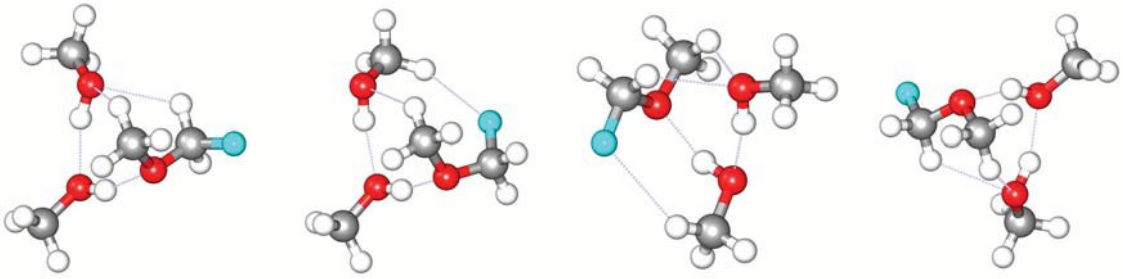

$e_1$: $\Delta BE$ = -66.92 $e_2$: $\Delta BE$ = -65.76 $e_3$: $\Delta BE$ = -64.57 $e_4$: $\Delta BE$ = -63.80

Figure 1: **$FCH_2OCH_3$ $\cdots$ $2CH_3OH$** (solvated ethers) structures for the fluorocarbene-(methanol)$_3$ system. All relative energies in kcal mol$^{-1}$, calculated at the CCSD(T)/6-311++G$(d,p)$//MP2/6-311++G$(d,p)$ level. Relative stability order within the ethers group is indicated by the subscript $n$ in $e_n$. QTAIM predicted intermolecular hydrogen interactions are represented by dotted lines.

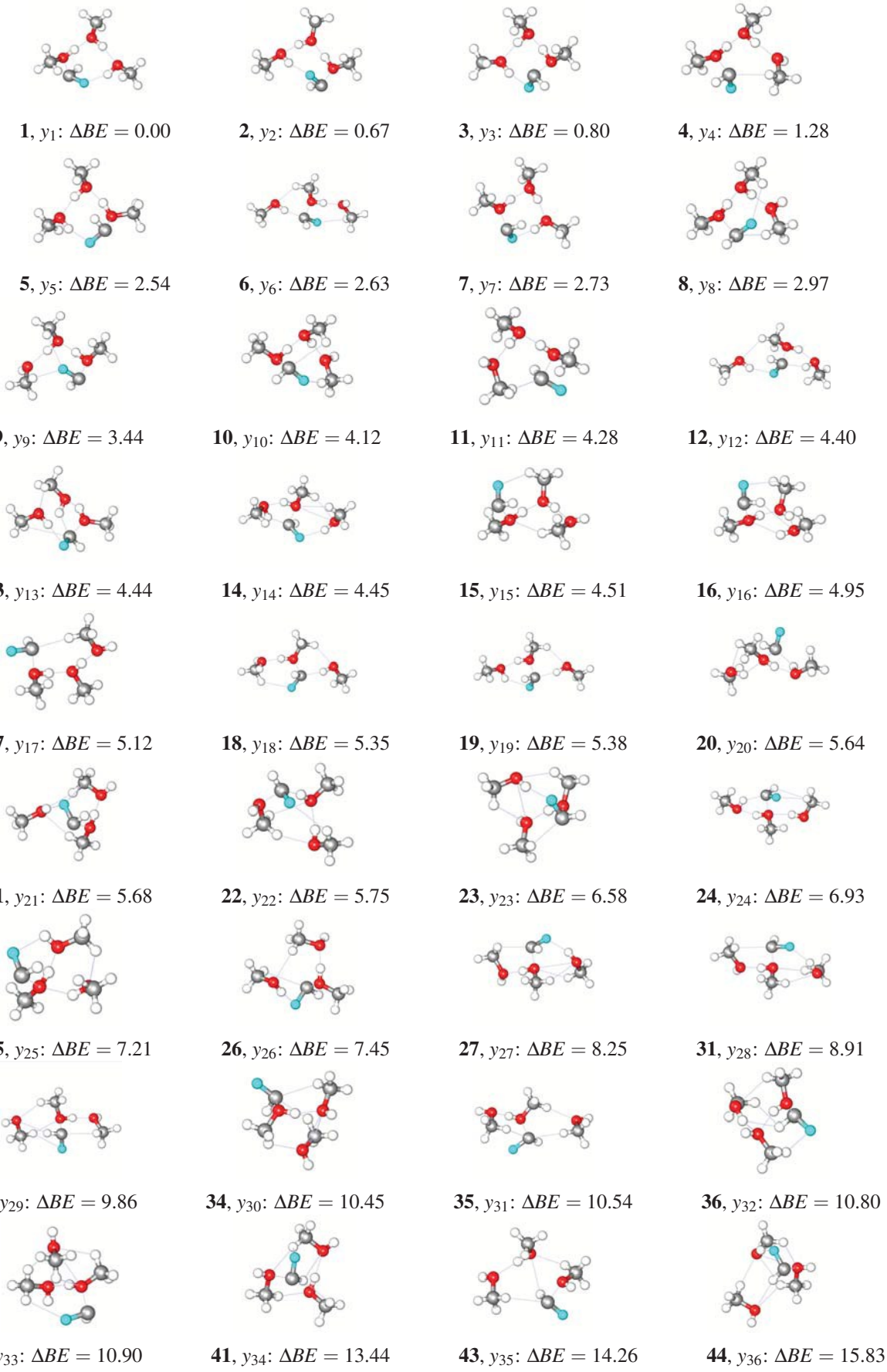


Figure 2: Structures for the fluorocarbene-(methanol)$_3$ ***O*-ylides**. Bold numbers indicate the ZPE corrected CCSD(T)/6-311++G$(d,p)$//MP2/6-311++G$(d,p)$ energy order among the mixing of the groups *O*-ylides and complexes, starting with **1** for the cluster having the lowest energy. Relative stability order within the *O*-ylides group is indicated by the subscript $n$ in $y_n$. All relative energies in kcal mol$^{-1}$. QTAIM predicted intermolecular hydrogen and Cc$\cdots$O interactions are represented by dotted lines.

**28**, $c_1$: $\Delta BE = 8.46$

**29**, $c_2$: $\Delta BE = 8.46$

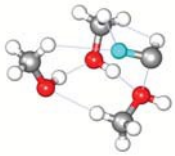

**32**, $c_4$: $\Delta BE = 9.76$

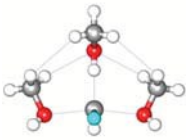

**37**, $c_5$: $\Delta BE = 10.82$

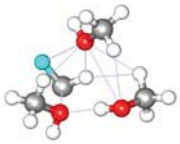

**39**, $c_6$: $\Delta BE = 12.48$

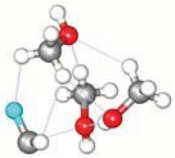

**40**, $c_7$: $\Delta BE = 12.70$

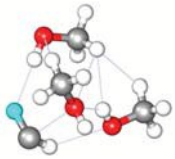

**42**, $c_8$: $\Delta BE = 14.19$

Figure 3: Structures for the fluorocarbene-(methanol)$_3$ ***O*-ylidic complexes**. Bold numbers indicate the ZPE corrected CCSD(T)/6-311++G$(d,p)$//MP2/6-311++G$(d,p)$ energy order among the mixing of the groups *O*-ylides and complexes, starting with **1** for the cluster having the lowest energy. Relative stability order within the *O*-ylidic complexes group is indicated by the subscript $n$ in $c_n$. All relative energies in kcal mol$^{-1}$. QTAIM predicted intermolecular hydrogen and Cc$\cdots$O interactions are represented by dotted lines.

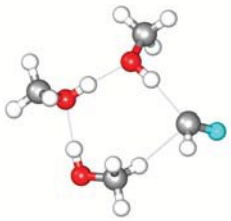

**30**, $c_3$: $\Delta BE = 8.62$

Figure 4: Hydrogen bonded complex. The cycle contains one secondary and three primary hydrogen bonds. There is no interaction between the electron donor O (methanol) and carbene carbon. Bold number indicates the ZPE corrected CCSD(T)/6-311++G$(d,p)$//MP2/6-311++G$(d,p)$ energy order among the mixing of the groups *O*-ylides and complexes, starting with **1** for the cluster having the lowest energy. Relative stability order within the *O*-ylidic complexes group is indicated by the subscript $n$ in $c_n$. Relative energy in kcal mol$^{-1}$. QTAIM predicted intermolecular hydrogen interactions are represented by dotted lines.

We will refer to the 48 structures by inherent features of the resulting species. Table 1 lists clusters in decreasing order of stability according to the calculated CCSD(T)/6-311++G$(d,p)$ relative energies. In the notation, two criteria were used: $(a)$ Relative stability order within each group; $e_1$, ..., $e_4$, $y_1$, ..., $y_{36}$, and $c_1$, ..., $c_8$, in which $e_1$, $y_1$, and $c_1$ are the most stable species at the (MP2 ZPE-corrected) CCSD(T)/6-311++G$(d,p)$ level of theory for ethers, *O*-ylides, and *O*-ylidic complexes, respectively. $(b)$ Global relative stability order; 1,...,44, in which 1 is the most stable at the (MP2 ZPE-corrected) CCSD(T)/6-311++G$(d,p)$ level of theory for the set of the *O*-ylides, and *O*-ylidic complexes groups. Table 1 also shows binding energies (*BE*), relative binding energies ($\Delta BE$), isomer populations estimated via standard Boltzmann distribution analysis using the Gibbs free energies, and Cc$\cdots$O distances of interaction and Cc$\cdots$O bond orders for all clusters.

It is readily seen in Table 1 that there is a noticeable difference between binding energies for the solvated ether clusters ($e_n$) and the other solvated clusters (*O*-ylides ($y_n$) and *O*-ylidic complexes ($c_n$)). It is clear that the $e_n$ species correspond to products of carbene insertion into the O–H bond of methanol, surrounded by 2 extra methanol molecules. Relative to the isolated species (the fluorocarbene and the three methanol molecules), their binding energies (formation energies) are around 90 kcal mol$^{-1}$. Ethers constitute the most stable minima found.

For the remaining structures, it is possible to establish that although the stability does not seem to directly depend on the number of explicit interactions between solute and solvent (for example, see the structural complexity for the least stable structures $c_4$, $c_6$ and $c_7$ in Figure 3), the structures maximizing the number of primary hydrogen bonds have the lowest energies and sometimes include the fluorine atom as hydrogen bond acceptor. Roughly speaking, 3D geometrical motifs have the highest energies. In general terms, carbene carbon$\cdots$oxygen distances and bond orders are related to the stability order of the clusters. For non-ether structures such bond lengths are distributed into two ranges: 1.44-1.86 Å and 2.21-2.39 Å.

Table 1: Total ($BE$) and relative ($\Delta BE$) binding energies for F$\ddot{\text{C}}$H(MeOH)$_3$ clusters calculated at MP2/6–311++G$(d,p)$ or CCSD(T)/6–311++G$(d,p)$ levels of theory and corrected for the unscaled MP2/6–311++G$(d,p)$ ZPEs. $BE$s for ethers correspond to formation energies. All CCSD(T)/6–311++G$(d,p)$ calculations using the MP2/6–311++G$(d,p)$ optimized geometries. All energies in kcal/mol. Cc$\cdots$O distances (in Å) and Cc$\cdots$O WBI are intermolecular distances and Wiberg bond indexes between carbene carbon and the methanol oxygen, respectively. $\%x_i$ are the estimated Boltzmann populations within each group: $O$-ylides and complexes.

| Structure | Cc$\cdots$O distances | Cc$\cdots$O WBI | $BE$ CCSD(T) | $BE$ MP2 | $\Delta BE$ CCSD(T) | $\Delta BE$ MP2 | $\%x_i$ Gibbs[a] |
|---|---|---|---|---|---|---|---|
| **(FCH$_2$OCH$_3$)$\cdots$(2CH$_3$OH) Ethers** | | | | | | | |
| $e_1$ | 1.39 | 0.93 | -91.63 | -98.63 | -66.92 | -69.57 | |
| $e_2$ | 1.38 | 0.94 | -90.47 | -97.39 | -65.76 | -67.51 | |
| $e_3$ | 1.40 | 0.90 | -89.28 | -96.24 | -64.57 | -66.36 | |
| $e_4$ | 1.40 | 0.90 | -88.50 | -95.48 | -63.80 | -65.60 | |
| **HFC$^-$–$^+$OHCH$_3$$\cdots$(2CH$_3$OH) *O*-Ylides** | | | | | | | |
| **1**, $y_1$ | 1.55 | 0.63 | -24.70 | -29.88 | 0.00 | 0.00 | 54.34 |
| **2**, $y_2$ | 1.55 | 0.63 | -24.04 | -29.17 | 0.67 | 0.71 | 25.15 |
| **3**, $y_3$ | 1.61 | 0.57 | -23.91 | -29.07 | 0.80 | 0.82 | 3.55 |
| **4**, $y_4$ | 1.56 | 0.62 | -23.42 | -28.83 | 1.28 | 1.05 | 5.93 |
| **5**, $y_5$ | 1.58 | 0.59 | -22.17 | -27.18 | 2.54 | 2.70 | 0.59 |
| **6**, $y_6$ | 1.57 | 0.62 | -22.08 | -27.68 | 2.63 | 2.20 | 8.45 |
| **7**, $y_7$ | 1.59 | 0.58 | -21.98 | -26.94 | 2.73 | 2.95 | 0.33 |
| **8**, $y_8$ | 1.63 | 0.54 | -21.74 | -26.83 | 2.97 | 3.06 | 0.39 |
| **9**, $y_9$ | 1.57 | 0.60 | -21.27 | -26.30 | 3.44 | 3.58 | 0.09 |
| **10**, $y_{10}$ | 1.64 | 0.53 | -20.58 | -25.49 | 4.12 | 4.39 | 0.20 |
| **11**, $y_{11}$ | 1.65 | 0.52 | -20.42 | -25.34 | 4.28 | 4.54 | 0.10 |
| **12**, $y_{12}$ | 1.55 | 0.64 | -20.31 | -25.98 | 4.40 | 3.91 | 0.22 |
| **13**, $y_{13}$ | 1.57 | 0.61 | -20.26 | -25.84 | 4.44 | 4.04 | 0.13 |
| **14**, $y_{14}$ | 1.59 | 0.60 | -20.25 | -26.02 | 4.45 | 3.86 | 0.11 |
| **15**, $y_{15}$ | 1.59 | 0.58 | -20.20 | -25.18 | 4.51 | 4.71 | 0.08 |
| **16**, $y_{16}$ | 1.59 | 0.57 | -19.76 | -24.60 | 4.95 | 5.28 | 0.04 |
| **17**, $y_{17}$ | 1.66 | 0.51 | -19.59 | -24.43 | 5.12 | 5.46 | 0.02 |
| **18**, $y_{18}$ | 1.60 | 0.58 | -19.35 | -24.71 | 5.35 | 5.17 | 0.08 |
| **19**, $y_{19}$ | 1.59 | 0.59 | -19.33 | -24.61 | 5.38 | 5.28 | 0.05 |
| **20**, $y_{20}$ | 1.58 | 0.59 | -19.07 | -24.74 | 5.64 | 5.15 | 0.13 |
| **21**, $y_{21}$ | 1.58 | 0.59 | -19.03 | -23.73 | 5.68 | 6.15 | 0.02 |
| **22**, $y_{22}$ | 1.60 | 0.57 | -18.95 | -24.28 | 5.75 | 5.61 | 0.02 |
| **23**, $y_{23}$ | 1.44 | 0.60 | -18.13 | -22.88 | 6.58 | 7.00 | 0.00 |
| **24**, $y_{24}$ | 1.72 | 0.47 | -17.77 | -22.69 | 6.93 | 7.19 | 0.00 |
| **25**, $y_{25}$ | 1.60 | 0.56 | -17.50 | -22.12 | 7.21 | 7.77 | 0.00 |
| **26**, $y_{26}$ | 1.57 | 0.59 | -17.25 | -22.06 | 7.45 | 7.83 | 0.00 |
| **27**, $y_{27}$ | 1.63 | 0.54 | -16.45 | -20.97 | 8.25 | 8.92 | 0.00 |
| **31**, $y_{28}$ | 1.66 | 0.51 | -15.80 | -20.15 | 8.91 | 9.73 | 0.00 |
| **33**, $y_{29}$ | 1.67 | 0.51 | -14.84 | -19.37 | 9.86 | 10.51 | 0.00 |
| **34**, $y_{30}$ | 1.61 | 0.56 | -14.26 | -18.96 | 10.45 | 10.92 | 0.00 |
| **35**, $y_{31}$ | 1.66 | 0.51 | -14.17 | -18.74 | 10.54 | 11.14 | 0.00 |
| **36**, $y_{32}$ | 1.65 | 0.51 | -13.90 | -18.14 | 10.80 | 11.74 | 0.00 |
| **38**, $y_{33}$ | 1.62 | 0.54 | -13.80 | -18.30 | 10.90 | 11.58 | 0.00 |
| **41**, $y_{34}$ | 1.87 | 0.31 | -11.27 | -14.42 | 13.44 | 15.46 | 0.00 |
| **43**, $y_{35}$ | 1.67 | 0.48 | -10.45 | -14.62 | 14.26 | 15.27 | 0.00 |
| **44**, $y_{36}$ | 1.76 | 0.40 | -8.87 | -12.30 | 15.83 | 17.58 | 0.00 |
| **H–C̈–F$\cdots$(3CH$_3$OH) Complexes** | | | | | | | |
| **28**, $c_1$ | 2.31 | 0.09 | -16.25 | -18.11 | 8.46 | 11.77 | 7.04 |
| **29**, $c_2$ | 2.31 | 0.09 | -16.25 | -18.11 | 8.46 | 11.77 | 7.04 |
| **30**, $c_3$ | - | - | -16.08 | -18.20 | 8.62 | 11.68 | 83.36 |
| **32**, $c_4$ | 2.23 | 0.11 | -14.95 | -16.68 | 9.76 | 13.20 | 0.39 |
| **37**, $c_5$ | 2.39 | 0.07 | -13.89 | -16.31 | 10.82 | 13.58 | 2.15 |
| **39**, $c_6$ | 2.21 | 0.12 | -12.23 | -14.01 | 12.48 | 15.87 | 0.00 |
| **40**, $c_7$ | 2.28 | 0.10 | -12.00 | -13.73 | 12.70 | 16.16 | 0.02 |
| **42**, $c_8$ | 2.26 | 0.10 | -10.51 | -12.00 | 14.19 | 17.88 | 0.00 |

[a] MP2/6–311++G$(d,p)$ Gibbs free energies (298 K, 1 atm)

We can observe in Table 1 that MP2 and CCSD(T) give slightly different stabilization orderings and that MP2 overestimates stability. In general, $BEs$ per solvent molecule at the MP2/6-311++G$(d,p)$ level range between 4.00 and 9.96 kcal/mol, and between 2.96 and 8.23 kcal/mol per solvent molecule at CCSD(T)/6-311++G$(d,p)$ level. It is seen that energies per solvent molecule are large and comparable to typical hydrogen bond energies per solvent molecule in methanol clusters ($BE \approx 8.22$ kcal/mol per solvent molecule for the most stable tetramer cluster at CCSD(T) level)[39] and even in ethanol clusters ($BE \approx 3.60$ kcal/mol per solvent molecule for the most stable dimer cluster at CCSD(T) level).[66]

## Classification of clusters

An inspection at the highest energy structures in Table 1 (below structure $y_{27}$) indicates that from the purely energetic point of view, it is not totally clear where the borderline between the *O*-ylides and the *O*-ylidic complexes is. For those structures, there is no correlation between the Cc$\cdots$O distances and the CCSD(T) stability order, and some Cc$\cdots$O distances are intermediate between a typical case of *O*-ylide (around 1.5 Å,[21]) and a typical case of *O*-ylidic complex (larger than 2.0 Å[21,30]). Therefore, we need to address the problem of the theoretical distinction between these kinds of connected species. Another very important and related aspect is the study of the nature of the different species resulting from the PES exploration of the carbene-solvent systems. This last aspect could be useful to better appreciate the particular characteristics of the *O*-ylidic complexes with respect to other species. Accordingly, we categorize the 48 clusters into different groups by applying the following methods:

1. IUPAC defines ylides as compounds in which an anionic site $Y^-$ (carbon, in the case of carbenes) is attached directly to a heteroatom $X^+$ (oxygen, in the case of methanol) carrying a formal positive charge.[18] In the field of solvation and complexation of carbenes, the term *O*-ylides has been used to refer to species with conventional C–O distances, but not necessarily with formal charges or ionic nature. Instead, for *O*-ylides of the Cc-O type, the

charges are relative charges with respect to the case of the isolated molecules: the oxygen of methanol tends to lose (donate) electronic density in the ylide, with respect to the $CH_3OH$. On the other hand, Cc tends to gain electron density with respect to the isolated carbene.

Within NBO, $q(A)$, the natural charge on atom A, is given by the nuclear charge minus the sum of electronic natural populations of Natural Atomic Orbitals (NAOs) on the atom.[56] In Figure 5, $\Delta q(Cc)$ and $\Delta q(O)$ are defined as the relative natural charges of the carbene carbon and oxygen atom, respectively, in the resulting cluster, minus their corresponding natural charges in the isolated monomer, fluorocarbene and methanol, respectively. In this way, $\Delta q$ corresponds to a gain (- sign) or a loss (+ sign) of electrons.

As can be appreciated on the left panels of Figure 5, for the majority of structures (except for ethers) there is a gain of electron density at the carbene carbon, $\Delta q(Cc) < 0$. This is accompanied by the simultaneous loss of electron density at the oxygen atom for a group of structures. This loss of electron density for the methanol oxygen atom involved in the Cc$\cdots$O interaction (or, correlatively, the electron density gain on Cc), serves as an initial criterion to differentiate the nature of bonding between *O*-ylides ($\Delta q(O) > 0$) and *O*-ylidic complexes ($\Delta q(O) < 0$).

Besides the sign of $\Delta q$, it can be seen in Figure 5 that all clusters are grouped in three distinct arrays within particular ranges of Cc$\cdots$O Wiberg bond indices and distances. Bond orders approach 1 for single bonds and approach 0 for weak interactions while being near to 0.5 for partially formed/partially broken bonds, such as would be expected for ethers, *O*-ylidic complexes and *O*-ylides, respectively. This constitutes an additional basis for the distinction between *O*-ylidic complexes and *O*-ylides.

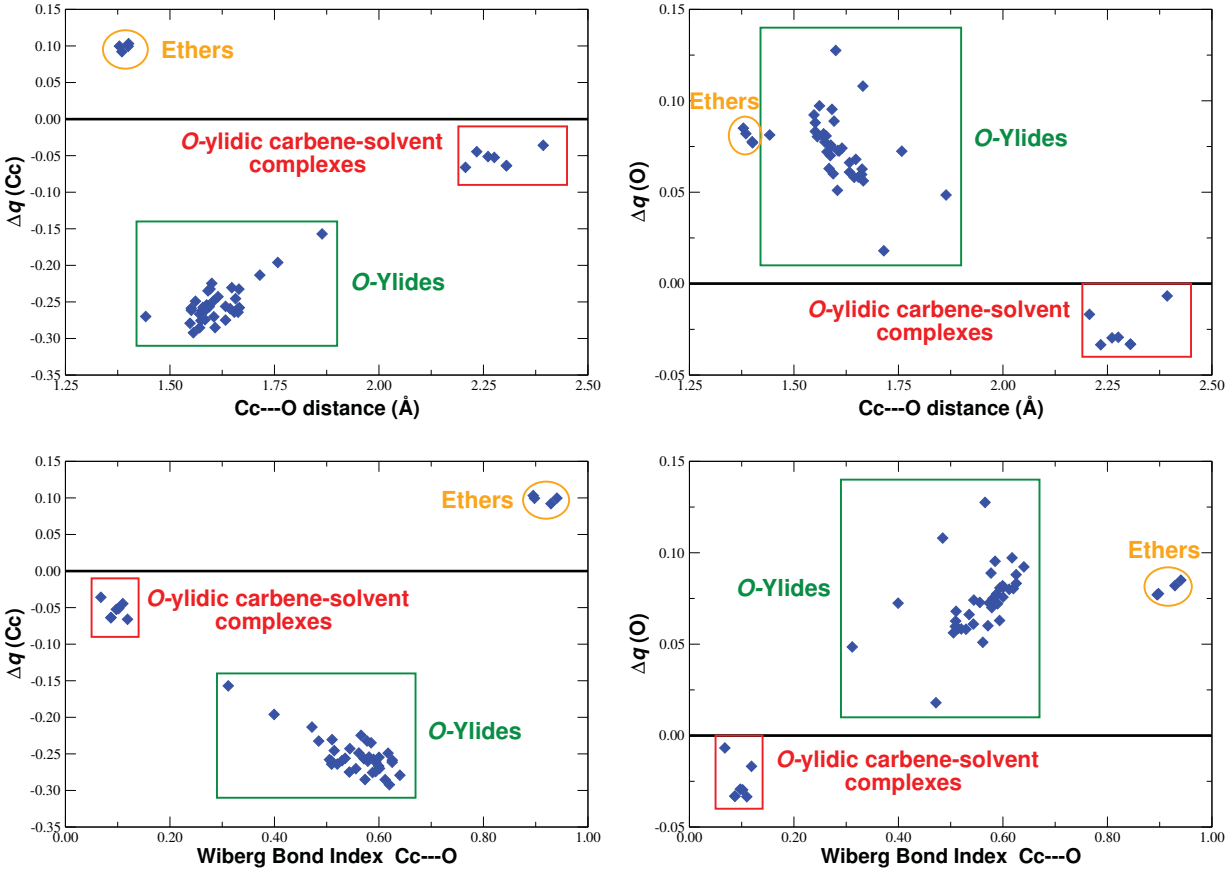


Figure 5: Relationships between the relative natural charges -on carbene carbon (left) and oxygen (right) atoms- and bond lengths (top) and bond orders (bottom) for all Cc···O intermolecular interactions in the fluorocarbene-(methanol)$_3$ systems. Distances in Å.

Another arresting deduction (Figure 6) is obtained between the relative natural charges and the CCSD(T) stability order. Clearly the fluorocarbene-(methanol)$_3$ relative stability issue is not an exclusive consequence of the exchange of electronic density between the Cc and O atoms: as it is seen in Figure 6, neither the sign nor the magnitude of $\Delta q$ correlate with cluster stability. The range of values of the CCSD(T) binding energies for *O*-ylides and *O*-ylidic complexes indicate that it is not possible to distinguish between the most energetic *O*-ylides and the *O*-ylidic complexes using these *BE* values (see Table 1 and Figure 6). This can be a consequence of the fact that hydrogen bonding networks (among solute-solvent and solvent-solvent) are very important in determining cluster stabilities. For example, for the highest energy ylides, $y_{34}$, $y_{35}$, $y_{36}$, the Cc···O contact is clearly conditioned by hydrogen

bonding networks which hold together these aggregates. Thus, we argue that, for the most energetic *O*-ylides cases, large Cc···O distances and small Cc···O Wiberg bond indices are dominated by the restrictions imposed at other areas of the structure. However, they present $\Delta q(O) > 0$ and $\Delta q(Cc) < 0$, which are inherent characteristic of the ylides.

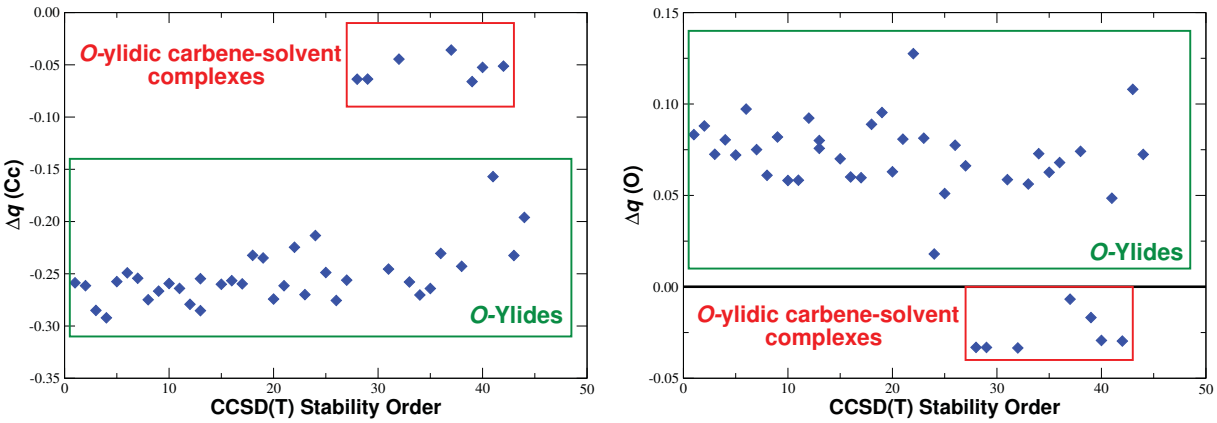


Figure 6: Relationships between the relative natural charges (on carbene carbon and oxygen atoms) and the CCSD(T) stabilities for all Cc···O intermolecular interactions in the fluorocarbene-(methanol)$_3$ clusters.

2. From NBO results, we found that for all structures exhibiting $\Delta q(O) > 0$, i. e., ethers and ylides, Cc···O contacts lead to $\sigma_{O-Cc}$ bonding orbitals. Thus, these are strong interactions and have certain single bond character, which is consistent with the Cc···O bond orders stated above. Particular examples of this type of NBOs are provided in Figure 7. All remaining structures are clusters where the Cc···O contact is just a $n_O \longrightarrow \sigma^*_{Cc-F}$ interaction. Such structures were classified as the *O*-ylidic complexes.

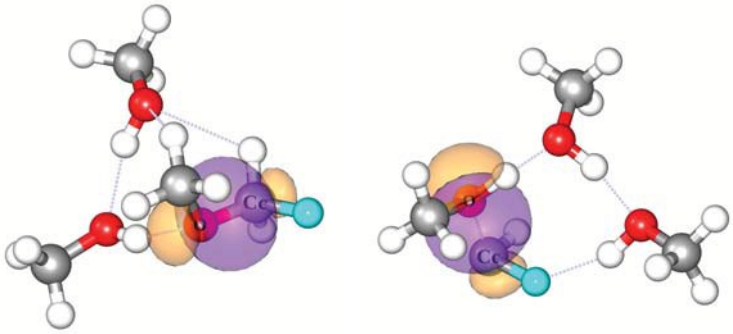

Figure 7: $\sigma_{O-Cc}$ orbital interactions involved in the Cc···O contacts. The cases for $e_1$ (left) and $y_1$ (right) are shown.

3. As shown in Figure 8, there is an expected correlation between distances and bond orders for the Cc···O pair. Nicely, it can be observed that the species are clearly defined, distributed in well separated groups by a gap, from 1.80 to 2.20 Å. Notice that the group that contains Cc···O distances larger than 2.20 Å, can be clearly categorized as specifically solvated *O*-ylidic complexes. At the top of Figure 8 the four insertion products are also noticed. It is possible to establish a distance limit between carbene carbon and oxygen, from which the carbene-solvent *O*-ylidic complexes and *O*-ylides can be distinguished. We found that 2.20 Å is the distance in the case of the systems studied here. Thus, structures with Cc···O distances larger than 2.20 Å are candidates to be fluorocarbene-methanol complexes.

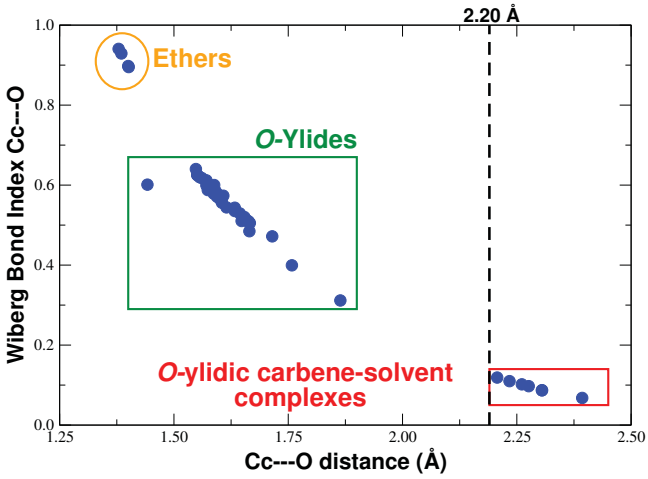


Figure 8: Wiberg bond indices vs. distances for carbene carbon···oxygen interaction in all FCH···$(MeOH)_3$ equilibrium structures. Bond lengths in Å.

In order to test the consistency of Wiberg bond indexes for our system and considering that the obtained values depend on the calculation method,[67] we used another type of bond order, namely, the natural bond order derived from the Natural Resonance Theory module of the NBO program.[56] For *O*-ylides, natural bond orders are somewhat larger than Wiberg indices, but the tendencies of the two bond orders agree with each other and groups are also differentiated. Results are shown in Appendix A0 of the supplementary material.

4. The values of the electron density, its Laplacian, and the $|\mathscr{V}(\mathbf{r}_c)|/\mathscr{G}(\mathbf{r}_c)$ ratio (Equation 1) at the BCPs are analyzed for all clusters as depicted in Figure 9, and Appendices A1 and A2 of

the supplementary material. It can be observed in Figure 9 that the clusters appear grouped in distinct ranges of electron density at BCPs, determining interactions of different nature or indirectly defininig the groups (see sections below for additional evidence to support this claim). For example, there is a marked difference among electron density values at BCPs for ethers and for the remaining structures. For *O*-ylides and *O*-ylidic complexes, there is a fuzzy borderline; we have already used some additional criteria to classify the structures of the border (see above discussion about atomic natural charges and NBO).

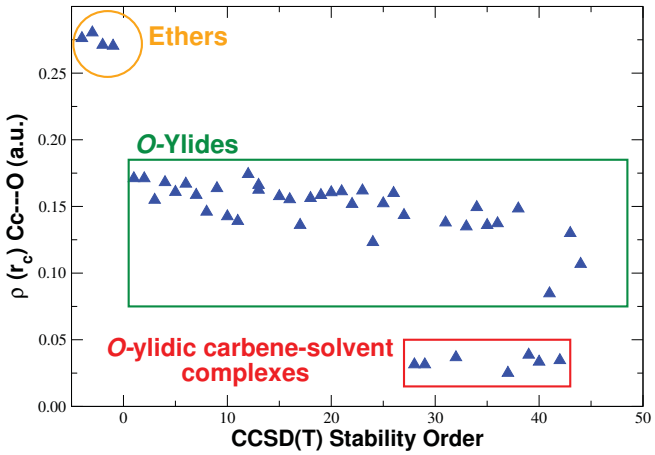


Figure 9: Electron density values at carbene carbon-oxygen BCPs vs stability order for all H–C̈–F + $3H_3C$–OH clusters.

Laplacians of electron density at BCPs for the Cc···O interactions are shown in Appendix A1 of the supplementary material. Again, certain groupings are remarkable, but it is not as when compared with the results of natural charges, bond orders, distances and orbitals. A set of 11 clusters can be distinguished as long range carbene carbon-oxygen interactions (small positive Laplacians). The remaining structures show negative Laplacians, thus Cc···O interactions with high degrees of covalency. Furthermore, it is possible to differentiate among structures with $\nabla^2\rho(\mathbf{r}_c) < 0$, since they are grouped into two arrays having very different Laplacian range of values at carbene carbon – oxygen BCPs. One of those groups consists of the four ethers and the other is the *O*-ylides.

As can be expected, for species representing *O*-ylidic metastable complexes, the interactions between solvent molecules (through MeOH electron donor oxygen atoms) and carbene carbon, are not covalent ($\nabla^2\rho(\mathbf{r}_c) > 0$), but they have some covalent character, as we will see below. However, among these, there are four special structures, each one enclosed by a maroon ellipse (see Appendix A1 in the supplementary material), with characteristics of *O*-ylide under NBO results. Therefore, there are only seven well defined complexes (see Figure 3).

Figure 9 and Figure in Appendix A1 also show that the stability order is not directly correlated with the Laplacian nor with the electron density values at Cc$\cdots$O BCPs. This constitutes additional support to the view exposed above regarding the importance of hydrogen bonds in determining the cluster structural arrangements, their stabilities, and the properties of the C$\cdots$O interactions.

Other properties studied for all clusters were the $|\mathscr{V}(\mathbf{r}_c)|/\mathscr{G}(\mathbf{r}_c)$ and $\mathscr{H}(\mathbf{r}_c)/\rho(\mathbf{r}_c)$ ratios (Equation 1), as a strategy to quantify the degree of covalency of Cc$\cdots$O bonding. The results can be found in Appendix A2 of the supplementary material for carbene carbon$\cdots$oxygen BCPs. It is seen that the group cataloged as fluorocarbene-methanol *O*-ylidic complexes presents the lowest ratios, $1.2 > |\mathscr{V}(\mathbf{r}_c)|/\mathscr{G}(\mathbf{r}_c) > 0.9$, characteristic of closed shell (weak interactions) with certain covalent character, but not formally covalent. The other structures, namely, insertion products and most of the ylides, display $|\mathscr{V}(\mathbf{r}_c)|/\mathscr{G}(\mathbf{r}_c) > 2$, indicative of a covalent or shared interaction. For ethers and *O*-ylides the $|\mathscr{V}(\mathbf{r}_c)|/\mathscr{G}(\mathbf{r}_c)$ ratios are very different. They appear as two well defined groups, where ethers have higher values (more strength and covalent character between carbene carbon and oxygen). Structures located at the edges of the groups (enclosed into maroon ellipses in Figure of Appendix A2) have intermediate covalency. All the above information, and that included in supplementary material, reveals that it is possible to distinguish the species by their Cc$\cdots$O bonding nature, by means of analysis of their properties at BCPs.

*Brief analysis of the groups*

**Insertion Products:** Four different mechanisms have been proposed (one of them[68,69] depicted in Appendix A3 of the supplementary material), to describe the chemical transformations when carbenes react with molecules bearing the O–H bond. The final product is an ether or an alcohol depending on whether alcohol or water molecules are used.[70] In our case, the products are fluoromethylethers, $e_n$, they are listed in Table 1 and shown in Figure 1 with labels **(FCH$_2$OCH$_3$)$\cdots$(2CH$_3$OH)**.

The group of ethers contains four stable structures, characterized by a non-planar network of hydrogen bonds. Fluoromethylether interacts with two extra methanol molecules, via two primary hydrogen bonds and at least two secondary hydrogen bonds. Furthermore, all Cc$\cdots$O interactions in these insertion products are formal bonds under NBO (see the left side of Figure 7).

From QTAIM and WBI results, it can be seen that Cc$\cdots$O bond orders for the ether products are about 0.9 (a single bond) and their Cc$\cdots$O distances are around $\sim$1.4 Å, which is comparable with typical covalent bond lengths for C–O, around 1.43 Å. They have $|\mathscr{V}(\mathbf{r}_c)|/\mathscr{G}(\mathbf{r}_c) > 2.3$, $\mathscr{H}(\mathbf{r}_c)/\rho(\mathbf{r}_c) < 0$, $\nabla^2\rho(\mathbf{r}_c) < 0$ (see Appendix A1 and A2) and $\rho(\mathbf{r}_c)$ values larger than 0.25 at carbene carbon$\cdots$oxygen BCPs. Therefore, they should be characterize as covalent bonds.

**Ylides:** An extensive variety of possibilities leads to a rich conformational space for ylides as can be noticed in Figure 2. This group comprises 32 structures which are characterized by the typical structures containing the polar Cc$\cdots$O bond, but where the H of methanol has not been transferred yet (to form the final ether). The lowest energy ylides have a network of primary hydrogen bonds, but no secondary hydrogen bonds (see structures $y_1$, $y_2$ and $y_3$ in Figure 2); in this way, molecules participating in the network leave their respective $CH_3$ groups free from cluster interactions. Secondary hydrogen bonds have a smaller stabilizing effect than primary hydrogen bonds in clusters of this type, because when its number becomes significant respect to the number

of primary hydrogen bonds (see structures **28, 38** and **36** in Figure 2), clusters appear to be more energetic.

Covalent Cc$\cdots$O bond lengths of true *O*-ylide molecules are around 1.5 Å.[21] In this work, for ylides, all Cc$\cdots$O interactions lead to $\sigma_{Cc-O}$ bonding orbitals (see the right side of Figure 7), and cover the range from 1.42 Å to 1.67 Å distances (see Figure 8 and Table 1). Laplacian values for the *O*-ylides are negative (in some cases very near to zero) as depicted in Appendix A1, and their $|\mathscr{V}(\mathbf{r}_c)|/\mathscr{G}(\mathbf{r}_c)$ and $\mathscr{H}(\mathbf{r}_c)/\rho(\mathbf{r}_c)$ ratios are larger than 2 and smaller than 0, respectively, indicating that the interaction between carbene carbon and methanol oxygen is covalent (see Appendix A2). Regarding WBIs for Cc$\cdots$O bonds, a 0.45-0.65 interval is seen, electron densities at C$\cdots$O BCPs remain in the 0.12-0.18 a.u. interval. For this group $\Delta q(O) > 0$ and $\Delta q(Cc) < 0$ when natural charges in monomers are compared with natural charges calculated in the clusters: $\Delta q$ at carbene carbon, Cc, in the -0.14,-0.31 *e* range and $\Delta q$ covering the 0.05-0.14 *e* range for the oxygen atom.

*O*-ylides could be related to intermediate species[71] for reactions between carbenes and alcohol (or water) molecules, as shown in Appendix A3, just before TS is reached.

***O*-ylidic carbene-solvent complexes:** We located 7 structures in this group (see Figure 3). As a general rule, 3D geometrical preferences are observed. In most cases (except for structure 40, $c_7$ in Figure 3), fluorocarbene is interacting at the same time with all methanol molecules. Thus, we suggest that a larger number of contacts between the solute (carbene) and solvent (methanol) appears to confer stability to the complexes.

All intermolecular contacts between carbene carbon and methanol oxygen are caused by the interaction of an oxygen lone pair with a carbene antibonding orbital ($n_O \rightarrow \sigma^*_{Cc-F}$), but those never become a $\sigma$ orbital themselves (This issue will be extended in the NBO analysis for the

carbene-solvent complexes section). Such interactions have Laplacians larger than zero and $0.9 < |\mathscr{V}(\mathbf{r}_c)|/\mathscr{G}(\mathbf{r}_c) < 1.1$ ratios at BCPs. In addition, most complexes show $\mathscr{H}(\mathbf{r}_c)/\rho(\mathbf{r}_c) < 0$, denoting some degree of covalency. Similar conclusions regarding the sign of the Laplacian and Espinosa's criteria were reported in an earlier study about complexes among fluorocarbene amide and two THF molecules.[30]

The *O*-ylidic complexes exhibit $\Delta q(O)$ and $\Delta q(Cc)$ very close to zero (with ranges between -0.09 and -0.01 *e*, and -0.04 and 0.00 *e* respectively). This indicates weak long range interactions. With regard to the stabilization of the complexes, it is seen from Table 1 that the values of *BE*s are distributed within a range of 5.74 kcal/mol, covering the -16.25,-10.51 kcal/mol interval. In this way, structural isomers for carbene–solvent complexes are separated by very small energy gaps, leading to a complicated situation where most of the structures have signicant populations and the properties of these systems would comprise contributions from all clusters.

According to the information in Figure 8, *O*-ylidic carbene-solvent complexes show Cc$\cdots$O bond orders in a narrow range (0.05,0.14) and Cc$\cdots$O distances from 2.21 to 2.39 Å. Moss *et al.*[21] and Hadad *et al.*[30] have found resemblant carbene carbon – oxygen distance values for dichlorocarbene-THF complex at PBE/6-311+G(d) level (2.2 Å) and fluorocarbene amide-THF complexes at B97D/6-311++G$(d,p)$ level of theory (2.1 to 3.2 Å) respectively.

Given that Hadad and coworkers[30] proposed a unusual solvation through both p-orbital lobes of a carbene carbon, we added to our configuracional space search some complexes with highly symmetrical hand-constructed inicial structures. Only one symmetric structure was found, it is labeled as 38 in Figure 3. It seems to have $C_s$ symmetry. Although Hadad and coworkers stated *"the situation of having both-plane-sides double micro-solvated carbene carbon 'O-ylide complexes,' through the simultaneous interaction of each THF electron donor oxygen atom with its corresponding Cc p lobe, seems to confer a special stability to the system."*, the analysis

above (binding energies) indicates that the structure exhibiting simultaneous interaction with each oxygen of two methanol molecules is not the most stable structure within *O*-ylidic carbene-solvent complexes. Such seemingly anomalous finding, could be explained by appealing to the differences between the type of solvents employed in the microsolvation, tetrahydrofuran on one hand, and methanol on the other hand. Cluster stabilization in aggregates of MeOH can be understood by invoking the joint effect of cooperative polarization and cooperative charge transfer, it has been suggested that forces governing methanol cluster stabilization are thought to include dominant contributions from electrostatic interactions[39] and $n \longrightarrow \sigma^*$ interactions.[65] Therefore, in the case of microsolvation of fluorocarbene with three methanol solvent molecules, interactions between solvent molecules, mainly primary hydrogen bonds, have significantly high contributions in the stabilization of the complexes. Note that THF solvent molecules cannot afford primary hydrogen bond.

**Hydrogen bonded carbene-solvent complex:** It is defined by one structure which lacks the Cc$\cdots$O interaction between carbene carbon and methanol oxygen atom. This cluster is depicted in Figure 4. A similar complex has already been proposed as a type of carbene–solvent complex among methylchlorocarbene and anisole.[19] There are two consecutive primary methanol-methanol hydrogen bonds and the interaction of one C–H antibonding orbital, $\sigma^*_{C-H}$, as electron acceptor of the $\sigma$ carbene carbon occupied orbital.

In Table 1, isomer population results are differentiated by group. It can be seen that if temperature, entropy and internal degrees of freedom are included in the analysis, cyclic, more open, noncompact structures are preferred. The structures **1-8** in Figure 2, are within 2.97 kcal/mol at CCSD(T)/6-311++G($d$,$p$) level, accounting for $\sim$99% of the Boltzmann reference population within the ylides group, while structures $c_1$, $c_2$ and $c_3$, in Figure 3, show $\sim$97% in isomer population within the *O*-ylidic carbene-solvent complexes group. Note how close to each other the binding energies are, which means that several isomers have significant populations at standard conditions in both groups.

## NBO analysis for the carbene-solvent complexes

Another approach to gain insight into the nature of bonding interactions in fluorocarbene–methanol complexes is NBO analysis.[56] Our results suggest that two important features deserve to be highlighted:

($i$) In all complexes, there is a carbene carbon lone electron pair, $n_{Cc}^{(1)}$, in a hybrid orbital of around 60% $s-$character and 40% $p-$character, corresponding to the approximate description $2s$ and $2p$ NAOs on carbon.

($ii$) The empty $p-$like orbital of fluorocarbene is generally represented by a Cc–F antibonding orbital and consists basically in a linear combination of $2p_{Cc}$ and $2p_F$ NAOs, with predominance of $2p_{Cc}$ orbital.

Let us analyze the orbital interactions responsible for the stability in some selected complexes, namely, the lowest energy complex (Figure 10), the $C_s$ hand-constructed complex (Figure 11), the highest energy complex (Figure 12) and hydrogen bonded complex (Figure 13), labeled as **28**, $c_1$, **37**, $c_5$, **42**, $c_8$ and **30**, $c_3$, respectively, in Figure 3 and in Figure 4.

Figure 10 shows results of NBO analysis for the most stable *O*-ylidic carbene-solvent complex, $c_1$. In this system, it seems that networks of hydrogen bonds dictate cluster stabilization because NBO predicts very strong interactions from lone pairs in oxygen or carbene carbon atoms with O–H antibonding orbital of a solvent molecule, this is the typical stabilizing interaction in water clusters.[65] A pair of examples are displayed at the top panel of Figure 10 with interaction energies, $E^{(2)}$, of 8.84 and 13.08 kcal/mol. An additional orbital donor-acceptor contribution within the same complex is drawn at the bottom panel of Figure 10, with interaction energy of 21.06 kcal/mol. It represents the specific solvation by electron density donation from solvents having nonbonding electrons, in this case methanol, to the *p*-like carbene carbon orbital.

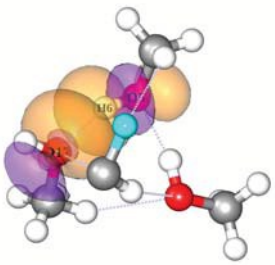

$n^{(1)}_{O17} \longrightarrow \sigma^{*}_{O5-H6}$ **= 8.84 kcal/mol**

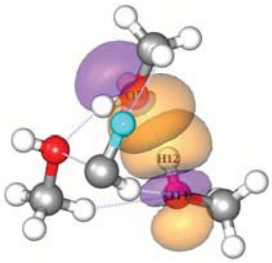

$n^{(2)}_{O5} \longrightarrow \sigma^{*}_{O11-H12}$ **= 13.08 kcal/mol**

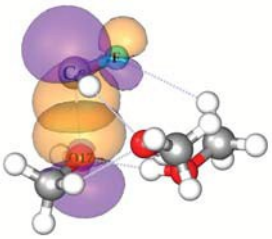

$n^{(2)}_{O17} \longrightarrow \sigma^{*}_{Cc-F}$ **= 21.06 kcal/mol**

Figure 10: Orbital interactions defining cluster stabilization for the structure labeled as **28**, $c_1$ in Figure 3. This is the most stable flourocarbene–(methanol)$_3$ complex.

In the $C_s$ hand constructed structure, the leading interaction is the Cc lone pair (donor) to O20–H21 antibonding orbital (acceptor), with $E^{(2)} = 34.65$ kcal/mol, as shown at the left side of Figure 11. There are two interactions in second order of importance: $n^{(2)}_{O14} \longrightarrow \sigma^{*}_{Cc-F}$ and $n^{(2)}_{O8} \longrightarrow \sigma^{*}_{Cc-F}$, corresponding to interactions between lone electron pairs orbitals of the two methanol oxygen atoms and the empty orbital $p-$like orbital of carbene carbon. As the Cc$\cdots$O distances are the same at each side of molecular plane of fluorocarbene, 2.39 Å, both interactions have the same $E^{(2)} = 16$ kcal/mol (right side in Figure 11).

Figure 12 depicts donor-acceptor interaction in cluster **42**, $c_8$. For this structure, structural complexity can be summarized by ascending order of importance as secondary hydrogen bonds with very little orbital overlap, –F$\cdots$H–OMe interaction, primary hydrogen bonds between solvent molecules ($E^{(2)}$ around 3.90 kcal/mol, bottom panel in Figure 12) and orbital interactions between lone pair from methanol oxygen atom and the $p-$like orbital of Cc, i.e., $n^{(2)}_{O5} \longrightarrow \sigma^{*(1)(2)}_{Cc-F}$ with 10.94 and 8.54 kcal/mol stabilization energies.


Figure 11: Orbital interactions defining the cluster stabilization for structure labeled as **37**, $c_5$ in Figure 3. This cluster corresponds to a proposed structure, "hand constructed" structure.

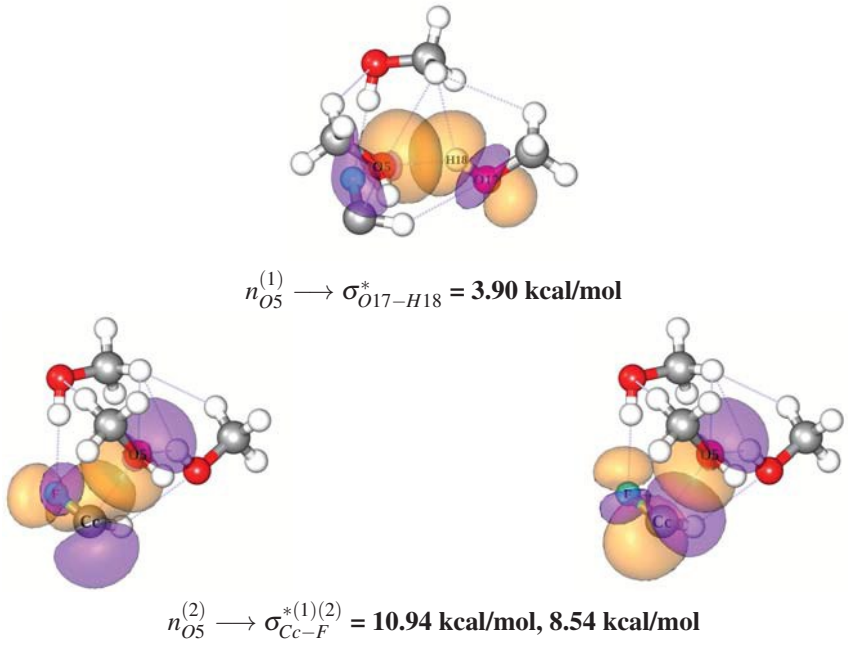


Figure 12: Orbital interactions defining the cluster stabilization for structure labeled as **42**, $c_8$ in Figure 3. This complex corresponds to the highest energy structure.

The case of the hydrogen bonded complex is very interesting, because although it is not an *O*-ylidic complex, it is the second most stable within the group of the complexes. In fact, it has the largest isomer population into the complexes group (83.36%) when Gibbs free energies are considered. Orbital interactions for that complex are displayed in Figure 13. For this structure, interaction energies of primary hydrogen bonds are relatively high (see top panel, Figure 13), with

$n_{Cc}^{(1)} \longrightarrow \sigma_{O11-H12}^{*}$ exhibiting the largest effect in cluster stabilization. An interesting observation is that in this six-membered cycle, the only secondary hydrogen bond has a not negligible interaction energy, 1.50 kcal/mol, although quite small when compared to the others.

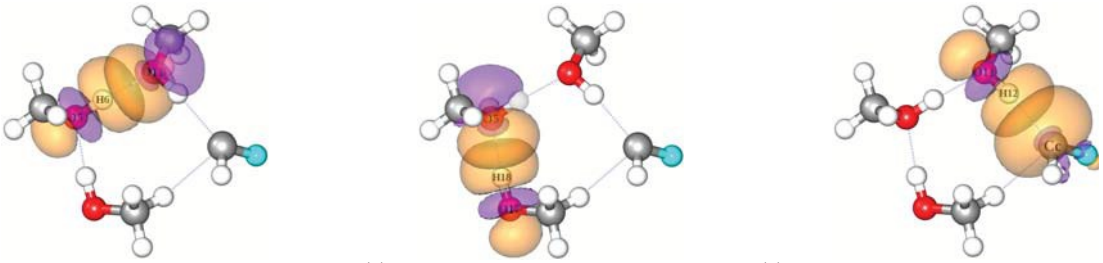


$n_{O11}^{(2)} \longrightarrow \sigma_{O5-H6}^{*}$ **= 17.77 kcal/mol** $n_{O5}^{(2)} \longrightarrow \sigma_{O17-H18}^{*}$ **= 13.73 kcal/mol** $n_{Cc}^{(1)} \longrightarrow \sigma_{O11-H12}^{*}$ **= 23.96 kcal/mol**

Figure 13: Orbital interactions defining the cluster stabilization for structure labeled as **30**, $c_3$ in Figure 4. This structure corresponds to hydrogen bonded complex.

At this point it is important to observe that in all the clusters examined here, the $n_{Cc} \longrightarrow \sigma_{O-H}^{*}$ interaction between the carbene carbon lone pair and any O-H antibond contributes significantly to the stabilization of the complexes. In fact, when this orbital interaction is not present, the complexes become higher in energy as in structure **42**, $c_8$ case (Figure 12). In addition, interactions between solute (carbene) and solvent (three methanol molecules) through lone pair orbitals of MeOH oxygen atoms and empty $p-$like orbitals of fluorocarbene represent $\approx 50$ % of second-order perturbative estimates of donor-acceptor (bond-antibond) interactions as can be seen in Figure 11.

From the point of view of NBO, our results show that hydrogen-bonding networks involving O–H groups from methanol molecules play a very important role in the stabilization of the complexes. Therefore, geometrical motifs in those clusters respond to a large extent to an arrangement dictated by hydrogen-bonding networks, comparable to the role played by $n_O \longrightarrow p-$like orbital of fluorocarbene. This situation may be very different in the case of the solvents which do not have the ability to form hydrogen bonds. In those complexes, the formation of stable clusters will be dictated by the Cc$\cdots$O interaction.

# Concluding Remarks

We summarize our findings as follows:

1. An exhaustive MP2/6–311++G($d,p$) exploration of the interaction possibilities implied in the singlet spin state of FCH(MeOH)$_3$ system results in the formation of 4 type of species: ethers, *O*-ylides, *O*-ylidic like solvation complexes and hydrogen bonded carbene-solvent complexes. Those species can be distinguished and studied using a combination of theoretical descriptors based on NBO and QTAIM methods and of relevant bond distances. Especially useful as distinction tools between *O*-ylides and *O*-ylidic complexes are the Cc$\cdots$O range of distances, the Cc$\cdots$O bond orders, the Cc$\cdots$O bond nature, and the natural charges on the carbene carbon, Cc, and methanol oxygen, O, in the clusters with respect to their natural charges in the isolated monomers.

2. In general, the structural preferences in the PES of the fluorocarbene + 3 methanol system, are mainly guided by the process of ether formation, the development of strong and weak interactions of the Cc$\cdots$O type, and the formation of hydrogen bond interactions of Cc$\cdots$H–O type (between the carbene molecule and the solvent molecules), and of O$\cdots$H–O type (among the solvent molecules).

3. The theoretical analysis reveals a fully formed $\sigma_{Cc-O}$ bonding orbital for all ethers and *O*-ylides and Cc$\cdots$O interactions with significant degree of orbital overlap between the $n_O$ and $\sigma^*_{Cc-F}$ ($p-$empty Cc) orbitals in the case of the *O*-ylidic complexes. Binding energies per solvent molecule in the case of the *O*-ylidic complexes are comparable to *BEs* in of H-bonded clusters.

4. An important factor affecting the $\sigma_{Cc-O}$ bond strength (and their degree of covalency), the overall stability and the structures of the *O*-ylides species, is the formation of primary hydrogen bond networks among the methanol molecules. H-bond interactions among solvent molecules can be strong enough to take the *O*-ylides to the limit of stability and nature of the Cc$\cdots$O interaction (low degree of covalency) of the *O*-ylidic complexes. For this reason

it is important to identify the suitable theoretical tools to distinguish between *O*-ylides and *O*-ylidic complexes. Those theoretical tools were named above, at point (1).

5. For the FCH-$(MeOH)_3$ system the *O*-ylidic complexes are affected by 3 type of interactions of comparable strength: interactions between the lone electron pairs of methanol oxygen (electron donor) and the empty $p-$like orbital of carbene carbon (electron acceptor), $n_O \longrightarrow \sigma^*_{Cc}$. The formation of hydrogen bond interactions of two types; Cc$\cdots$H–O; between the lone electron pair of the $\sigma-$like Cc orbital (electron donor) and the antibonding $\sigma-$like orbital of the HO group of methanol ($n_{Cc} \longrightarrow \sigma^*_{O-H}$), and O$\cdots$H–O; between the lone electron pairs of methanol oxygen (electron donor) and the antibonding $\sigma-$like orbital of the OH group of methanol ($n_O \longrightarrow \sigma^*_{O-H}$). Therefore, in the case of solvent molecules capable of forming H-bonds, the structure and Cc$\cdots$O strength of *O*-ylidic complexes could be affected by the formation of those H-bond interactions. In fact, we found a stable structure connected only via H-bonds, lacking the Cc$\cdots$O interaction.

6. For the systems studied here, binding energies indicate that the structure exhibiting both-plane side simultaneous interaction with oxygen atoms from two methanol molecules (double solvation through both *p* lobes of Cc), although stable, is not the most stable structure within *O*-ylidic carbene-solvent complexes. Probably three methanol molecules are not enough to complete the solvation shell of the flourocarbene, which makes more difficult to find very stable doubly solvated complexes. The formation of H-bonded networks and the H-bond cooperative stabilization are crucial aspects for the structure in this case. With few solvent molecules, it is not possible to achieve a good representation of the solvation in the bulk of the solution.

**Acknowledgements** We are grateful to Universidad de Antioquia for the financial support of this work through Estrategia de Sostenibilidad 2015-2016 and CODI project Nº 644. SG thanks the University of Antioquia for the graduate scholarship.

**Supporting information**: Cartesian coordinates for all optimized clusters reported in this work and additional analyisis about interactions.

## References


(1) Jones, M.; Moss, R. A. *"Carbenes"*; Wiley: New York, **1973**, *I*, 179.

(2) Jones, M.; Moss, R. A. *"Carbenes"*; Wiley: New York, **1975**, *II*, 235.

(3) Buchner, E.; Feldman, L. *Eur. J. Inorg. Chem*. **1903**, *3*, 3509–3517.

(4) Arduengo, A. J.; Davidson, F.; Dias, H. V. R.; Goerlich, J. R.; Khasnis, D.; Marshall, W. J.; Prakasha, T. K. *J. Am. Chem. Soc.* **1997**, *119*, 12742

(5) Hoffmann, R. *"Molecular Orbitals of Transition Metal Complexes"*. Oxford, **2005**

(6) Hirai, K.; Itoh, T.; Tomioka, H. *Chem. Rev.* **2009**, *109*, 3275-3332

(7) Moss, R. A.; Platz, M. S.; Jones, M., Jr. *"Reactive Intermediate Chemistry"*. Wiley: New York, **2004**.

(8) Bertrand, G. *"Carbene Chemistry: From Fleeting Intermediates to Powerful Reagent"*. CRC Press, **2002**

(9) Brinker, U.H. *"Advances in Carbene Chemistry"*. Elsevier, Amsterdam, **2001**

(10) Gonzalez, C.; Restrepo-Cossio, A.; Marquez, M. Wiberg, K.; De Rosa, M. *J. Phys. Chem. A*, **1998**, *102*, 2732-2738.

(11) Hoijemberg, P.A.; Moss, R. A.; Krogh-Jespersen, K. *J. Phys. Chem. A* **2012**, *116*, 4745-4750

(12) Moss, R. A.; Wang, L.; Hoijemberg, P.A.; Krogh-Jespersen, K. *Photochemistry and Photobiology*. **2014**, *90*, 287-293.

(13) Wang, J.; Kubicki, J.; Gustafson, T. L.; Platz, M. S. *J. Am. Chem. Soc*. **2008**, *130*, 2304-2313.

(14) Tippmann, E. M.; Platz, M. S.; Svir, I. B.; Klymenko, O. V. *J. Am. Chem. Soc.* **2004**, *126*, 5750-5762.

(15) Schmitz, E.; Ohme, R. *Tetrahedron Lett.* **1961**, , 612-614

(16) Moss, R. A. *J. Org. Chem.* **2010**, *75*, 5773-5783

(17) Moss, R. A.; Turro, N. J. *"Kinetics and Spectroscopy of Carbenes and Biradicals"*, Platz, M. S., Ed.; Plenum: New York, **1990** pp 213.

(18) IUPAC. *Compendium of Chemical Terminology, 2nd ed. (the "Gold Book")*. Compiled by A. D. McNaught and A. Wilkinson. Blackwell Scientific Publications, Oxford **1997**. XML on-line corrected version: http://goldbook.iupac.org (2006-) created by M. Nic, J. Jirat, B. Kosata; updates compiled by A. Jenkins. ISBN 0-9678550-9-8

(19) Moss, R. A.; Tian, J.; Sauers, R. R.; Krogh-Jespersen, K. *J. Am. Chem. Soc*. **2007**, *129*, 10019-10028.

(20) Moss, R. E.; Wang, L.; Weintraub, E.; Krogh-Jespersen, K. *J. Phys. Chem. A*. **2008**, *112*, 4651-4659

(21) Moss, R.; Wang A. L.; Odorisio, C. M.; Zhang, M.; Krogh-Jespersen, K. *J. Phys. Chem. A* **2010**, *114 (1)*, 209-217

(22) Moss, R. A. *J. Phys. Org. Chem.* **2011**, *24*, 866-875

(23) Tomioka, H.; Ozaki,Y.; Izawa, Y. *Tetrahedron* **1985**, *41*, 4987-4993

(24) Ruck, R. T.; Jones, M. Jr. *Tetrahedron Lett.* **1998**, *39*, 2277-2280

(25) Moss, R. A.; Yan, S.; Krogh-Jespersen, K. *J. Am. Chem. Soc.* **1998**, *120*, 1088-1089

(26) Krogh-Jespersen, K.; Yan, S.; Moss, R. A. *J. Am. Chem. Soc.* **1999**, *121*, 6269-6274

(27) Hoijemberg, P.A.; Moss, R. A.; Krogh-Jespersen, K. *J. Phys. Chem. A* **2012**, *116*, 358-363

(28) Moss, R.; Wang A. L.; Odorisio, C. M.; Krogh-Jespersen, K. *Tetrahedron Lett.* **2010**, *51*, 1467-1470

(29) González, C.; Restrepo, A.; Márquez, M.; Wiberg, K. *J. Am. Chem. Soc.* **1996**, *118(23)*, 5408-5411

(30) Hadad, C.Z.; Jenkins, S.; Flórez, E. *J. Chem. Phys*. **2015**, *142*, 094302.

(31) Pérez, J. F.; Restrepo, A. *"ASCEC V-02: Annealing Simulado con Energía Cuántica"*. Property, development and implementation: Theoretical Chemical Physics Group, Chemistry Institute, University of Antioquia: Medellín, Colombia. **(2008)**

(32) Pérez, J. F.; Flórez, E.; Hadad, C. Z.; Fuentealba, P.; Restrepo, A. *J. Phys. Chem. A* **2008**, *112 (25)*, 5749-5755.

(33) Pérez, J. F.; Hadad, C. Z.; Restrepo, A. *International Journal of Quantum Chemistry* **2008**, *108 (10)*, 1653-1659.

(34) Metrópolis, N.; Rosenbluth, A.; Rosenbluth, M.; Teller, A.; Teller, E. *J. Chem. Phys*. **1953**, *21*, 1087-1092.

(35) Kirkpatrick, S.; Gelatt, C.; Vecchi, M. *Science*. **1983**, *220*, 671-680.

(36) Restrepo, A.; Mari, F.; Gonzalez, C.; Marquez, M. *Química, Actualidad y Futuro*. **1995**, *5*, 101-112.

(37) Murillo, J.; David, J.; Restrepo, A. *Phys. Chem. Chem. Phys*. **2010**, *12*, 10963-10970.

(38) Gómez, S.; Guerra, D.; David, J.; Restrepo, A. *J. Mol. Model*. **2013**, *19*, 2173-2181.

(39) David, J.; Guerra, D.; Restrepo, A. *J. Phys. Chem. A*. **2009**, *113*, 10167-10173.

(40) Ramírez, F.; Hadad, C. Z.; Guerra, D.; David, J.; Restrepo, A. *Chem Phys Lett*. **2011**, *507*, 229-233.

(41) Echeverri, A.; Moreno, N.; Restrepo, A.; Hadad, C. *Chem. Phys. Lett.*. **2014**, *615*, 16-20.

(42) Guerra, D.; David, J.; Restrepo, A. *J. Comput. Meth. Sci. Eng*. **2014**, *14*, 93-102.

(43) Hincapié, G.; Acelas, N.; Castano, M.; David, J.; Restrepo, A. *J. Phys. Chem. A*. **2010**, *114*, 7809-7814.

(44) Ibargüen, C.; Manrique-Moreno, M.; Hadad, C. Z.; David, J.; Restrepo, A. *Phys. Chem. Chem. Phys*. **2013**, *15*, 3203-3211.

(45) Ibargüen, C.; Guerra, D.; Hadad, C. Z.; J.; Restrepo, A. *RSC Advances*. **2014**, *4*, 58217-58225.

(46) Zapata-Escobar, A.; Manrique-Moreno, M.; Guerra, D.; Hadad, C.; Restrepo, A. *J. Chem. Phys*. **2014**, *140*, 184312.

(47) Hadad, C.; Florez, E.; Merino, G.; Cabellos, J.L.; Ferraro, F.; Restrepo, A. *J. Phys. Chem. A*. **2014**, *118*, 5762-5768.

(48) Acelas, N.; Hincapié, G.; Guerra, D.; David, J.; Restrepo, A. *J. Chem. Phys.*. **2013**, *139*, 044310.

(49) Hadad, C.; Restrepo, A.; Jenkins, S.; Ramírez, F.; David, J. *Theor. Chem. Acc*. **2013**, *132*, 132.

(50) Gonzalez, J.D.; Florez, E.; Romero, J.; Reyes, A.; Restrepo, A. *J. Mol. Model*. **2013**, *19*, 1763-1777.

(51) Yepes, D.; Kirk, S.R.; Jenkins, S.; Restrepo, A. *J. Mol. Model*. **2012**, *18*, 4171-4189.

(52) David, J.; Guerra, D.; Restrepo, A. *Chem. Phys. Lett*. **2012**, *539-540*, 64-69.

(53) Romero, J.; Reyes, A.; David, J.; Restrepo, A. *Phys. Chem. Chem. Phys*. **2011**, *13*, 15264-15271.

(54) David, J.; Guerra, D.; Hadad, C.Z.; Restrepo, A. *J. Phys. Chem. A*. **2010**, *114*, 10726-10731.

(55) AIMAll (Version 14.04.17), Todd A. Keith, TK Gristmill Software, Overland Park KS, USA, **2014** (available in: http://aim.tkgristmill.com)

(56) Glendening, E. D.; Badenhoop, J.K.; Reed, A.E.; Carpenter, J.E.; Bohman, J.A.; Morales, C.M.; Landis, C.R.; Weinhold, F. *NBO, 6.0.* Theoretical Chemistry Institute, University of Wisconsin: Madison, WI, **2013**.

(57) Moss, R.; Wang A. L.; Odorisio, C. M.; Krogh-Jespersen, K. *J. Am. Chem. Soc.* **2010**, *132*, 10677-10679.

(58) Pople, J.; Head-Gordon, M.; Raghavachari, K. *J. Chem. Phys*. **1987**, *87*, 5968-5975.

(59) Gaussian 09, Revision D.01, M. J. Frisch, et al. Gaussian, Inc., Wallingford CT, **2009**.

(60) Bader, R. *Atoms In Molecules: A Quantum Theory*; Clarendon Press: Oxford, **1994**.

(61) Yang, Y. *J. Phys. Chem. A*. **2012**, *116*, 10150-10159.

(62) Merino, G.; Vela, A.; Heine, T. *Chem. Rev*. **2005**, *105*, 3812-3841.

(63) Espinosa, E.; Alkorta, I.; Elguero, J.; Mollins, E. *J. Chem. Phys*. **2002**, *117*, 5529-5542.

(64) Wiberg, K. *Tetrahedron*. **1968**, *24*, 1083-1096.

(65) Reed, A. E.; Curtiss, L. A.; Weinhold, F. *Chem. Rev*. **1988**, *88*, 899-926.

(66) Vargas-Caamal, A.; Ortiz-Chi, F.; Moreno, D.; Restrepo, A.; Merino, G.; Cabellos, J.L. *Theor. Chem. Acc*. **2015**, *134*, 16.

(67) Yang, Y. *J. Phys. Chem. A*. **2010**, *114*, 13257-13267.

(68) Pliego, J.; De Almeida, W. *J. Phys. Chem A*, **1999**, *103*, 3904-3909.

(69) Marquez, M.; Marí, F.; Gonzalez, C.; Restrepo, A. *J. Phys. Chem. A*, **1999**, *103*, 6191-6199.

(70) Orrego, J.; Cano. H.; Restrepo, A. *J. Phys. Chem. A* **2009**, *113*, 6517-6523.

(71) Gómez, S.; Guerra, D.; López, J. G.; Toro-Labbé, A.; Restrepo, A. *J. Phys. Chem. A*. **2013**, *117*, 1991-1999.